Redox Cycles in Trimethylamine Dehydrogenase and Mechanism of Substrate Inhibition†

Peter Roberts,‡ Jaswir Basran,‡ Emma K. Wilson,‡ Russ Hille,§ and Nigel S. Scrutton*,‡

Department of Biochemistry, University of Leicester, Adrian Building, University Road, Leicester LE1 7RH, United Kingdom, and Department of Medical Biochemistry, The Ohio State University, Columbus, Ohio 43210

Received June 18, 1999; Revised Manuscript Received August 17, 1999

ABSTRACT: The steady-state reaction of trimethylamine dehydrogenase (TMADH) with the artificial electron acceptor ferricenium hexafluorophosphate (Fc^+) has been studied by stopped-flow spectroscopy, with particular reference to the mechanism of inhibition by trimethylamine (TMA). Previous studies have suggested that the presence of alternate redox cycles is responsible for the inhibition of activity seen in the high-substrate regime. Here, we demonstrate that partitioning between these redox cycles (termed the 0/2 and 1/3 cycles on the basis of the number of reducing equivalents present in the oxidized/reduced enzyme encountered in each cycle) is dependent on both TMA and electron acceptor concentration. The use of Fc^+ as electron acceptor has enabled a study of the major redox forms of TMADH present during steady-state turnover at different concentrations of substrate. Reduction of Fc^+ is found to occur via the 4Fe-4S center of TMADH and not the 6-*S*-cysteinyl flavin mononucleotide: the direction of electron flow is thus analogous to the route of electron transfer to the physiological electron acceptor, an electron-transferring flavoprotein (ETF). In steady-state reactions with Fc^+ as electron acceptor, partitioning between the 0/2 and 1/3 redox cycles is dependent on the concentration of the electron acceptor. In the high-concentration regime, inhibition is less pronounced, consistent with the predicted effects on the proposed branching kinetic scheme. Photodiode array analysis of the absorption spectrum of TMADH during steady-state turnover at high TMA concentrations reveals that one-electron reduced TMADH—possessing the anionic flavin semiquinone—is the predominant species. Conversely, at low concentrations of TMA, the enzyme is predominantly in the oxidized form during steady-state turnover. The data, together with evidence derived from enzyme-monitored turnover experiments performed at different concentrations of TMA, establish the operation of the branched kinetic scheme in steady-state reactions. With dimethylbutylamine (DMButA) as substrate, the partitioning between the 0/2 and 1/3 redox cycles is poised more toward the 0/2 cycle at all DMButA concentrations studied—an observation that is consistent with the inability of DMButA to act as an effective inhibitor of TMADH.

Trimethylamine dehydrogenase (TMADH;[1] EC 1.5.99.7) is an iron−sulfur-containing flavoprotein isolated from the bacterium *Methylophilus methylotrophus* W_3A_1. The enzyme catalyzes the oxidative demethylation of trimethylamine (TMA) to dimethylamine (DMA) and formaldehyde (*1*):

$$(CH_3)_3N + H_2O \rightarrow (CH_3)_2NH + CH_2O + 2H^+ + 2e^-$$

The enzyme is a homodimeric protein having a subunit molecular mass of 83 kDa. Each subunit contains a covalently linked 6-*S*-cysteinyl FMN cofactor and a bacterial ferredoxin-type 4Fe-4S center; each subunit also possesses 1 equiv of tightly bound ADP of unknown function (*1*−*7*) but which probably represents a vestigial remnant of an ancestral dinucleotide-binding domain (*7*, *8*). The physiological electron acceptor for TMADH is an electron-transferring flavoprotein (ETF) (*9*), comprising a $\alpha\beta$ dimer of molecular mass 62 kDa. ETF possesses 1 equiv of FAD and 1 equiv of AMP; the function of AMP remains unclear (*10*). ETF-bound FAD cycles between oxidized and (anionic) semiquinone oxidation states (*9*) and therefore acts physiologically as a one-electron acceptor of TMADH, although two-electron reduction of ETF can be achieved electrochemically (*11*).

Full reduction of TMADH requires three electrons per subunit, two for reduction of the FMN and a third for reduction of the 4Fe-4S center, but only two reducing equivalents are removed from substrate during catalysis. The distribution of reducing equivalents within the two-electron reduced enzyme generated by reduction with excess substrate favors the formation of flavin semiquinone and reduced 4Fe-4S center, with the magnetic moments of the two paramag-

† This work was funded by the Royal Society and the UK Biotechnology and Biological Sciences Research Council. N.S.S. is a Lister Institute Research Fellow.

* Corresponding author: Telephone +44 116 223 1337; Telefax +44 116 252 3369; email nss4@le.ac.uk.

‡ University of Leicester.

§ The Ohio State University.

[1] Abbreviations: TMADH, trimethylamine dehydrogenase; ETF, electron-transferring flavoprotein; PMS, phenazine methosulfate; DCPIP, dichlorophenolindophenol; Fc^+, ferricenium hexafluorophosphate; TMA, trimethylamine; DEMA, diethylmethylamine; EDMA, ethyldimethylamine; DMButA, dimethylbutylamine; DMA, dimethylamine; TMAC, tetramethylammonium chloride; FMN, flavin mononucleotide; FAD, flavin adenine dinucleotide; EPR, electron paramagnetic resonance.

10.1021/bi9914098 CCC: $18.00
Published on Web 10/23/1999

Scheme 1: Proposed Branching Mechanism for TMADH[a]

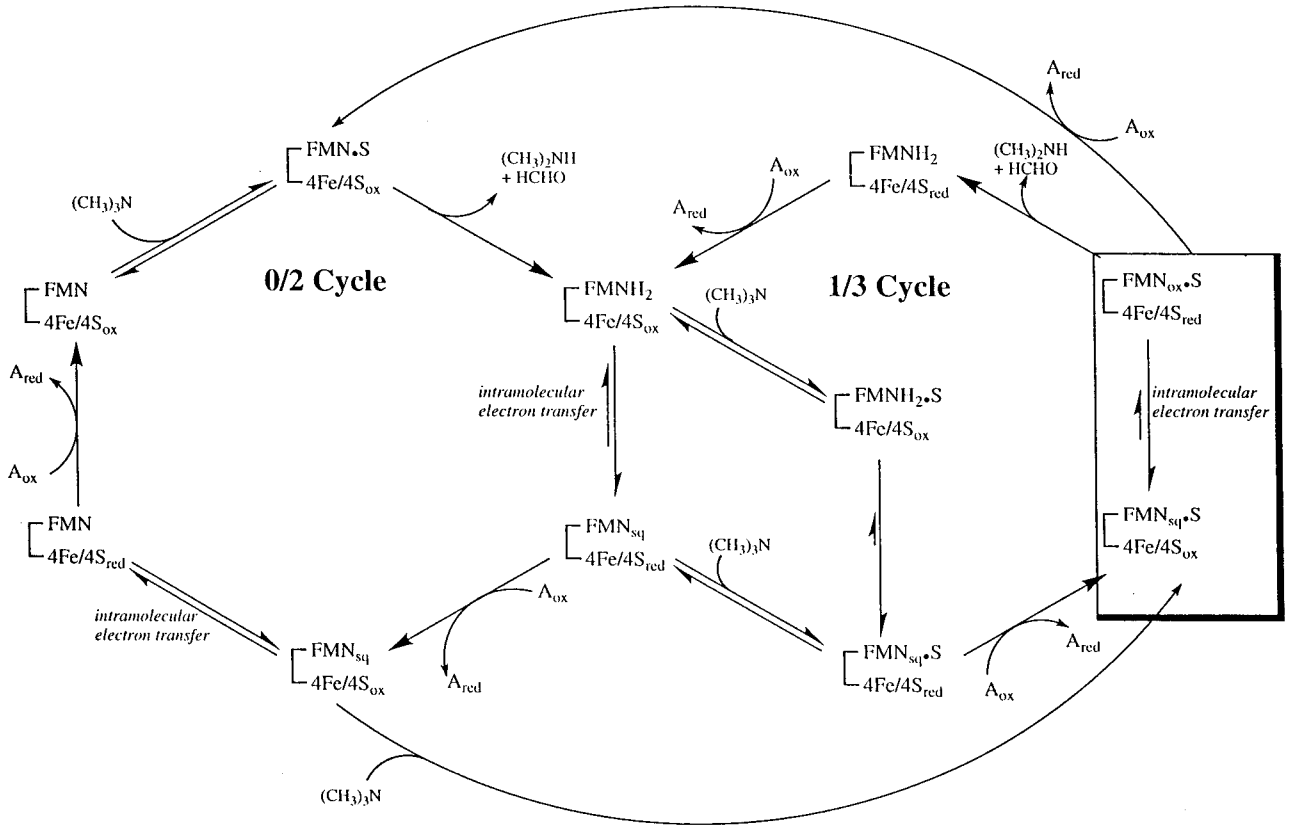

[a] In the 0/2 cycle, enzyme turns over between oxidized and two-electron reduced states; in the 1/3 cycle, enzyme turns over between one- and three-electron reduced states. Population of the 1/3 cycle leads to substrate inhibition of TMADH. The electron acceptor is represented by A.

netic centers interacting strongly to give a spin-interacting state (a triplet state). This triplet state is distinguished by a complex EPR signal centered near $g \sim 2$ and an unusually intense half-field $g \sim 4$ signal (*12*−*16*). Reduction of enzyme with dithionite in the presence of the substrate analogue and inhibitor tetramethylammonium chloride (TMAC) or by titration with dithionite at high pH also generates this characteristic spin-interacting state.

Previous stopped-flow and freeze-quench EPR kinetic studies have demonstrated that the reaction of TMADH with TMA or the slow substrate DEMA consists of three kinetic phases (*12*−*17*). On the basis of this work, an overall reductive half-reaction mechanism for TMADH has been proposed (*17*, *18*). The fast phase represents the two-electron reduction of the flavin cofactor (or, alternatively, formation of a covalent substrate−flavin adduct possessing an absorption spectrum comparable to that of reduced flavin) following cleavage of a C−H bond in one of the substrate methyl groups. The precise mechanism of C−H bond breakage remains unclear, but available evidence favors homolysis of the bond (*19*). The intermediate phase reflects the intramolecular electron transfer from reduced flavin to the 4Fe-4S center, generating flavin semiquinone and reduced iron−sulfur center. The slow phase involves dissociation of product and binding of a second substrate molecule, which perturbs the electron distribution in the partially reduced enzyme to facilitate formation of the spin-interacting state.

TMADH exhibits an unusual dependence on substrate concentration in steady-state reactions (*16*, *20*), being inhibited at high concentrations of TMA with either ETF or phenazine methosulfate (PMS) as electron acceptors. The mechanism of substrate inhibition has been debated. One mechanism posits an inhibitory substrate binding site distinct from the catalytically effective binding site (*20*), although there is no independent evidence for the existence of such an additional substrate binding site (*21*, *22*). Alternatively, we have suggested that TMADH can utilize two alternate catalytic cycles (*23*), cycling between oxidized and two-electron reduced enzyme (a 0/2 cycle) or one- and three-electron reduced enzyme (a 1/3 cycle), as depicted in Scheme 1. This situation arises because substrate donates two electrons, while ETF (or artificial acceptors such as PMS) takes up only one electron, and the enzyme itself can take up as many as three electrons. This model predicts that at low concentrations of TMA and/or high concentrations of oxidizing substrate, the 0/2 cycle predominates, and conversely at high [TMA] and/or low [oxidant], the 1/3 cycle is more important. The key to understanding excess substrate inhibition according to this model lies in the expectation that enzyme turnover in the 1/3 cycle, predominating at high concentrations of TMA, is expected to be slower than that in the 0/2 cycle. This is due to the fact that substrate binding stabilizes the semiquinone form of the flavin in one-electron reduced enzyme (*24*). Thus, binding of substrate to the partially reduced enzyme forms that accumulate in the steady-state under conditions of high substrate concentration must result in a redistribution of reducing equivalents, particularly in the case of $TMADH_{1e}$−, such that the flavin center becomes reduced (boxed equilibrium, Scheme 1). In this situation, oxidation of the bound substrate cannot occur because the flavin is not able to accept a pair of reducing equivalents from substrate. The kinetic effect is equivalent

to excess substrate inhibition but, significantly, does not involve a second inhibitory substrate-binding site. An analogous mechanism has also been shown to account for the excess substrate inhibition observed with xanthine oxidase (*25*). In this paper, we present spectroscopic and kinetic evidence for the operation of Scheme 1 in steady-state reactions of TMADH and provide a mechanistic framework for understanding substrate inhibition in TMADH.

EXPERIMENTAL PROCEDURES

Enzymes and Materials. Ferricenium hexafluorophosphate was synthesized as described by Lehman et al. (*26*). Wild-type TMADH was purified from *Methylophilus methylotrophus* W_3A_1 as described by Steenkamp and Mallinson (*1*), incorporating the modifications of Wilson et al. (*27*). The concentrations of wild-type TMADH (per subunit) were determined spectrophotometrically at 443 nm ($\epsilon = 27\,300$ M^{-1} cm^{-1}; *6*). The Y442G mutant TMADH was isolated and purified as described by Wilson et al. (*28*). The enzyme as isolated possesses its full complement of 4Fe-4S center and ADP, but a significant portion of the enzyme lacks the flavin. By use of spectrophotometric methods reported elsewhere (*29*), the fraction of flavinylated enzyme in the Y442G preparations used in the present study was estimated as approximately 25%. As only the flavinylated portion of the recombinant protein is catalytically active, only this portion of the total enzyme contributes to the absorbance changes seen in the experiments reported here. The concentration of the Y442G mutant of TMADH was determined by use of an effective extinction coefficient (19 000 M^{-1} cm^{-1} at 443 nm) for oxidized enzyme, calculated from the extent of the spectral change elicited by excess substrate (only the flavinylated enzyme is reducible by substrate).

Kinetic Assays. Steady-state kinetic measurements were performed in 20 mM potassium phosphate buffer, pH 7.0, with a 1-cm light path in a final volume of 1 mL. The desired concentrations of TMA and Fc^+ were obtained by making microliter additions from stock solutions to the assay mix. Reactions were initiated by the addition of Fc^+, and the reaction followed by the decrease in absorption at 300 nm due to reduction of Fc^+ ($\epsilon = 4300$ $M^{-1}cm^{-1}$) with a Hewlett-Packard 8452A single-beam diode array spectrophotometer. All data were collected at 30 °C. Some experiments required the use of high concentrations of TMA (>100 mM), which is positively charged at pH 7.0. Control experiments in which the total ionic strength was maintained throughout the concentration range (by the addition of KCl at lower [TMA]) indicated no significant difference in steady-state behavior compared with those reactions performed without the addition of KCl. Data were fitted by the fitting program Grafit (*30*) to the following equation that describes substrate inhibition in TMADH (*20*, *31*):

$$v = \frac{\left(1 + \frac{b[S]}{K_i}\right)V_{max}}{1 + \frac{K_s}{[S]} + \frac{K_s}{K_i} + \frac{[S]}{K_i}} \quad (1)$$

where *b* is a factor by which the intrinsic maximum velocity is affected. The remaining terms have their usual meanings.

Stopped-Flow Spectroscopy. Stopped-flow experiments were performed on an Applied Photophysics SX.17MV stopped-flow spectrophotometer. Spectral monitoring of the redox-active centers in TMADH during single-turnover and steady-state reactions was performed with a photodiode array detector. Spectral deconvolution was performed by global analysis and numerical integration methods using PROKIN software (Applied Photophysics). For single-wavelength studies, data collected at 443 nm were analyzed by nonlinear least-squares regression on an Archimedes 410-1 microcomputer using Spectrakinetics software (Applied Photophysics). Experiments were performed by mixing TMADH contained in buffer of the desired pH with an equal volume of substrate present at the desired concentration in the same buffer. In single-turnover experiments, the concentration of limiting substrate (Fc^+) was minimally 10-fold greater than that of TMADH, thereby ensuring pseudo-first-order conditions. For each substrate concentration used, at least four replicate measurements were collected and averaged. Substrate-reduced TMADH is quite stable to reoxidation in aerobic environments (half-life about 50 min; *27*), and consequently these stopped-flow experiments were carried out under aerobic conditions. Studies of electron transfer from dithionite-reduced TMADH to Fc^+ were conducted anaerobically. The sample-handling unit of the stopped-flow instrument was contained within a glovebox (Belle Technology Ltd) as described (*32*).

The absorbance change at 443 nm for reduction of TMADH by substrate was essentially monophasic, with a single rate constant obtained from fits of the data to

$$A_{443} = Ce^{-k_{obs1}t} + b \quad (2)$$

where *C* is the amplitude of the phase and *b* is the final absorbance. As shown previously (*17*, *19*), the observed rate constants were found to exhibit hyperbolic dependence on substrate concentration and the reaction sequence was modeled as shown in the general scheme:

$$TMADH_{ox} + TMA \overset{K_d}{\rightleftharpoons} TMADH_{ox}{\cdot}TMA \xrightarrow{k_{red}} TMADH_{red} + P \quad (3)$$

Data were then fitted to obtain related K_d and k_{red} values from $k_{obs} = k_{red}[S]/(K_d + [S])$ (*33*). As for reactions performed with ETF, transients for the reoxidation of three-electron reduced TMADH and one-electron reduced, phenylhydrazine-inactivated TMADH by Fc^+ were biphasic. Rate constants were calculated as described previously (*23*).

Selective Inactivation of Redox-Active Centers in TMADH. The 6-*S*-cysteinyl FMN of TMADH was inactivated with phenylhydrazine to produce a redox-inert 6-*S*-cysteinyl FMN C4a phenyl adduct (*6*, *34*). Phenylhydrazine-inactivated TMADH solutions were made anaerobic in a tonometer equipped with a ground joint for the dithionite titration syringe, a sidearm cuvette, and a three-way stopcock valve with a male Luer connector. The sample was alternately evacuated and flushed with oxygen-free argon. Reduced samples were prepared by titration with an anaerobic dithionite solution, and the reaction was followed spectrophotometrically by monitoring the absorbance from 350 to 450 nm. The iron−sulfur center of TMADH was selectively

inactivated by treatment with Fc^+ at pH 10, essentially as described by Huang et al. (*23*). The protein (30 μM) was incubated with Fc^+ (3 mM) contained in 50 mM potassium borate buffer, pH 10, at room temperature for 3 h. Excess oxidant was removed by size-exclusion chromatography using Sephadex G-25 equilibrated in 20 mM potassium phosphate buffer, pH 7. It has been shown that TMADH treated in this way can be reduced by TMA but is unable to pass electrons on to the physiological electron acceptor, ETF (*23*).

RESULTS

Artificial Electron Acceptors and the Direction of Electron Flow in TMADH. In steady-state studies of TMADH, artificial electron acceptors are routinely used in place of the physiological acceptor ETF. This arises because of the constraints in using a protein molecule as a substrate in steady-state reactions—the concentrations of oxidizing substrate required for routine analysis make the use of ETF impracticable and, due to the large absorbance of ETF in the 450 nm region, frequently not feasible. PMS and dichlorophenolindophenol (DCPIP) have been used widely in previous studies of TMADH (*1*, *16*). However, their intense absorption in the visible region makes these acceptors unsuitable for studies in which spectral changes associated with the redox-active centers of TMADH are monitored in the course of an enzyme-monitored turnover experiment. For this reason, we have used Fc^+ as an alternative electron acceptor. This electron acceptor produces less interference than PMS in the informative regions of the visible spectrum (350−450 nm), enabling spectroscopic characterization of the enzyme during steady-state turnover (Figure 1). In using Fc^+, however, it is important to establish that, like ETF, electron transfer occurs via the 4Fe-4S center of TMADH and not the 6-*S*-cysteinyl FMN. In principle, the 6-*S*-cysteinyl-FMN, 4Fe-4S cluster, or both redox centers could donate an electron to Fc^+.

The physiological route of electron transfer in TMADH is from the 6-*S*-cysteinyl FMN to the 4Fe-4S center and then to ETF (*23*, *28*), but the possibility of direct electron transfer from the flavin to Fc^+ must be considered. To determine whether Fc^+ can reoxidize directly the flavin of TMADH, the 4Fe-4S center of TMADH was selectively inactivated as described previously (*23*). Upon reduction by substrate, the flavin center of Fc^+ -inactivated TMADH cannot be oxidized by Fc^+ in either steady-state or stopped-flow single-turnover experiments, indicating that Fc^+ can only accept electrons from the 4Fe-4S center of TMADH. Evidence for competent electron transfer from the 4Fe-4S center to Fc^+ was obtained by inactivating the 6-*S*-cysteinyl FMN by treatment with phenylhydrazine, thereby producing the redox-inert phenyl-4a adduct of the 6-*S*-cysteinyl FMN (see refs *23* and *28*). In this case, it was found that Fc^+ was able to reoxidize dithionite-reduced protein (11.7 μM), as followed at 300 nm by stopped-flow. Under the reaction conditions used (50 mM potassium phosphate buffer, pH 7, 25 °C), reduced phenylhydrazine-inactivated TMADH was able to rapidly reduce Fc^+ (at a concentration of 100 μM), with an observed rate constant for the fast phase of 407 ± 14 s^{-1}. These experiments demonstrate that Fc^+ accepts electrons only from the reduced 4Fe-4S cluster of TMADH and not from the 6-*S*-cysteinyl FMN, and in this regard the flow of electrons during catalysis is comparable to that seen with the physiological redox acceptor, ETF (*23*).

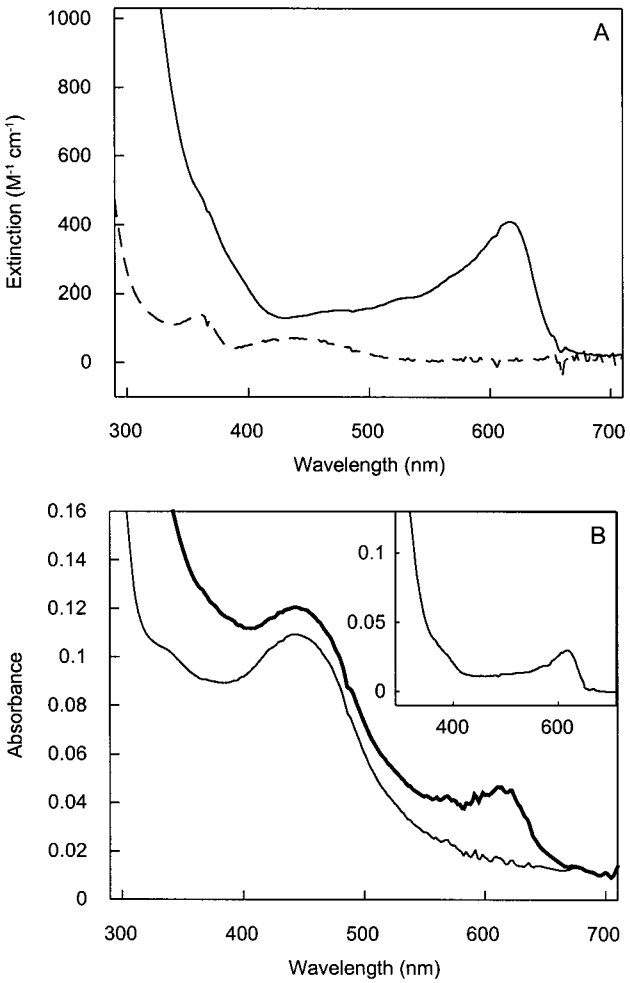

FIGURE 1: Spectra of oxidized and reduced Fc^+ and effects on the spectrum of oxidized TMADH. (A) Oxidized (solid line) and reduced (dashed line) Fc^+ in 20 mM potassium phosphate buffer, pH 7.0. (B) Spectrum of oxidized TMADH (4 μM) and oxidized TMADH (4 μM) plus Fc^+ (100 μM). (Inset) Difference spectrum showing contribution made by Fc^+.

Replacement of Tyr-442 by glycine on the surface of TMADH has been shown to substantially compromise electron transfer from TMADH to ETF (*28*). The precise role of Tyr-442 in native TMADH remains to be established, but its exchange for glycine both destabilizes the electron-transfer complex formed with ETF (with K_d increasing from 10 to 180 μM) and reduces the limiting rate constant for electron transfer within the TMADH·ETF complex, by about 30-fold (from 170 s^{-1} to 6 s^{-1}). It was of interest to investigate the ability of the Y442G mutant TMADH to reduce Fc^+. Any differential behavior with respect to electron-transfer rate between the wild-type and Y442G TMADH would establish that the productive binding site for Fc^+ is in this region of the protein. Samples of the wild-type and Y442G enzymes were each made anaerobic and fully reduced with dithionite as described (*23*). Each sample was then rapidly mixed with Fc^+ in the stopped-flow apparatus and reoxidation of the enzyme was monitored at 440 nm. This wavelength simultaneously monitors reoxidation of the 4Fe-4S center and the flavin. As expected—and as seen with ETF (*23*) as electron acceptor—the kinetic transients were more complex (approximated to biphasic

behavior), due to the sequential transfer of three electrons to Fc^+. However, the fast phase for each enzyme was clearly resolved from the rest of the absorbance changes. This first phase corresponds to a single electron transfer from the 4Fe-4S center of three-electron reduced TMADH to Fc^+.[2] From plots of the observed rate constant k_{obs} versus Fc^+ concentration, second-order rate constants of $(4.3 \pm 0.1) \times 10^6$ M^{-1} s^{-1} and $(2.3 \pm 0.03) \times 10^6$ M^{-1} s^{-1} were calculated for wild-type and Y442G TMADH, respectively (Figure 2). The data indicate that Tyr-442 plays only a modest role in facilitating electron transfer to Fc^+. The substantially larger effect with ETF (300-fold as compared to Fc^+) most likely reflects the specific role of Tyr-442 in directing specific protein−protein interactions during formation of the TMADH·ETF electron-transfer complex.

Steady-State Assays with Fc^+ as Electron Acceptor. Because prolonged incubation (over several hours) of TMADH with Fc^+ at pH 10 leads to inactivation of the enzyme (*23*), the possibility of enzyme inactivation is a major concern in any experiment that makes use of Fc^+ as electron acceptor. The success of any assay procedure depends on whether inactivation by Fc^+ can be prevented or suppressed on the time scale of the assay. At pH 7.0, preincubation of TMADH and Fc^+ for about 30 s prior to the addition of TMA does indeed reduce the observed initial velocity compared with reactions initiated by addition of Fc^+. Loss of activity increases with incubation time, indicating that preincubation with Fc^+ effects an irreversible inactivation of TMADH. However, when assays are initiated by adding Fc^+ or enzyme, the measured rates are linear over the time course of the experiment (typically between 30 and 60 s), contrary to the curvilinear traces expected for progressive inactivation of TMADH. Moreover, linear traces were obtained irrespective of the Fc^+ concentration, indicating that enzyme inactivation is negligible under the assay conditions employed. In the steady-state analyses described below, all reactions were initiated by the addition of Fc^+ to avoid inactivation of TMADH.

As originally reported by Steenkamp and Beinert (*16*), TMADH is inhibited by high concentrations of the physiological substrate TMA with PMS and DCPIP as electron acceptors. As shown in Figure 3, the same is found to be true when Fc^+ is used as oxidant. As with PMS and DCPIP, the degree of substrate inhibition is also affected by the Fc^+ concentration: at low Fc^+ concentrations, inhibition is more pronounced, whereas at high Fc^+ concentrations, the degree of inhibition is less marked. This observation is consistent with a mechanism in which substrate inhibits enzyme by formation of a catalytically nonproductive complex with partially reduced enzyme (Scheme 1). In this mechanism, high concentrations of Fc^+ will favor partitioning into the 0/2 redox cycle rather than the catalytically compromised 1/3 cycle.

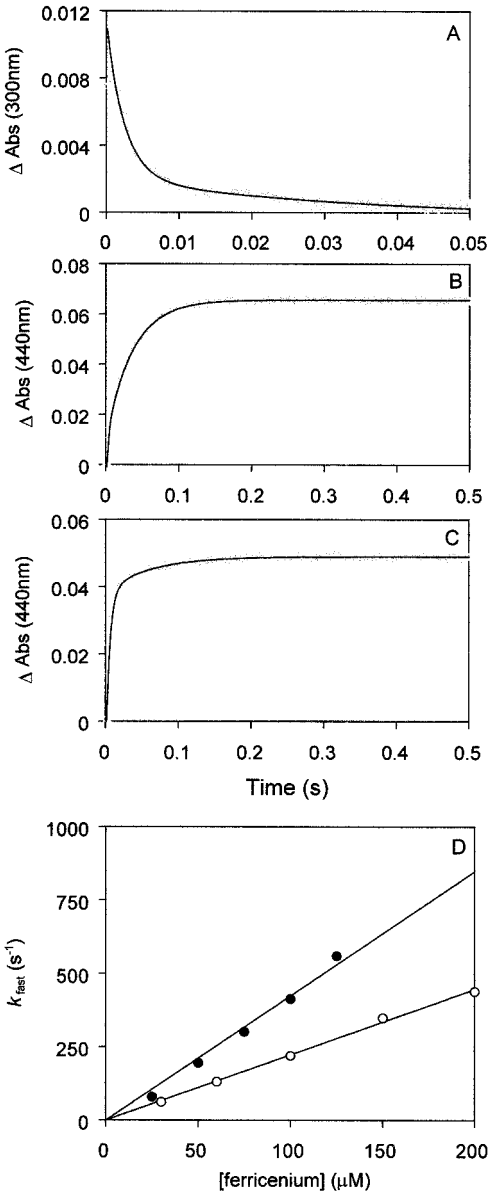

FIGURE 2: Transients and plots of the rate of electron transfer from the 4Fe-4S center of dithionite-reduced TMADH as a function of Fc^+ ion concentration for the wild-type and Y442G enzymes. (A) Transient observed at 300 nm for the reaction of phenylhydrazine-inactivated TMADH (4 μM) and Fc^+ (100 μM), $k_{fast} = 407$ s^{-1}; (B) transient observed at 440 nm for dithionite-reduced (three-electron reduced) TMADH (4 μM) and Fc^+ (100 μM), $k_{fast} = 423$ s^{-1}, $k_{slow} = 28$ s^{-1}; (C) transient observed at 440 nm for dithionite-reduced (fully reduced) Y442G TMADH (4 μM) and Fc^+ (100 μM), $k_{fast} = 220$ s^{-1}, $k_{slow} = 17$ s^{-1}. (D) Rate constants (fast phase) for the electron transfer from dithionite-reduced TMADH (three-electron reduced) and Y442G TMADH (fully reduced) to Fc^+ calculated from the absorbance changes at 440 nm by fitting to a double-exponential process: (●) observed rate constants for the wild-type enzyme; (○) observed rate constants for the Y442G mutant enzyme. The data were used to calculate second-order rate constants of $(4.2 \pm 0.1) \times 10^6$ M^{-1} s^{-1} and $(2.3 \pm 0.03) \times 10^6$ M^{-1} s^{-1} for the wild-type and Y442G mutant TMADH reactions, respectively. For all panels, the reaction components were contained in 50 mM potassium phosphate buffer, pH 7, and reactions were conducted at 25 °C.

Other, nonphysiological substrates for TMADH were also examined for excess substrate inhibition. Of the substrates investigated, ethyldimethylamine (EDMA), diethylmethylamine (DEMA), and triethylamine (TEA) were all found

[2] This phase was assigned to electron transfer from the 4Fe-4S center on the basis of the spectral change associated with this phase of the reaction for the wild-type and mutant protein. The amplitude of this phase contributed about 70% of the total absorbance change for the Y442G mutant and 25% for the wild type. The difference in amplitude is expected because the Y442G mutant is isolated as a mixture of flavinylated (~25%) and deflavo (~75%) enzyme and therefore only a relatively small proportion of the Y442G enzyme sample is reduced at the level of three electrons.

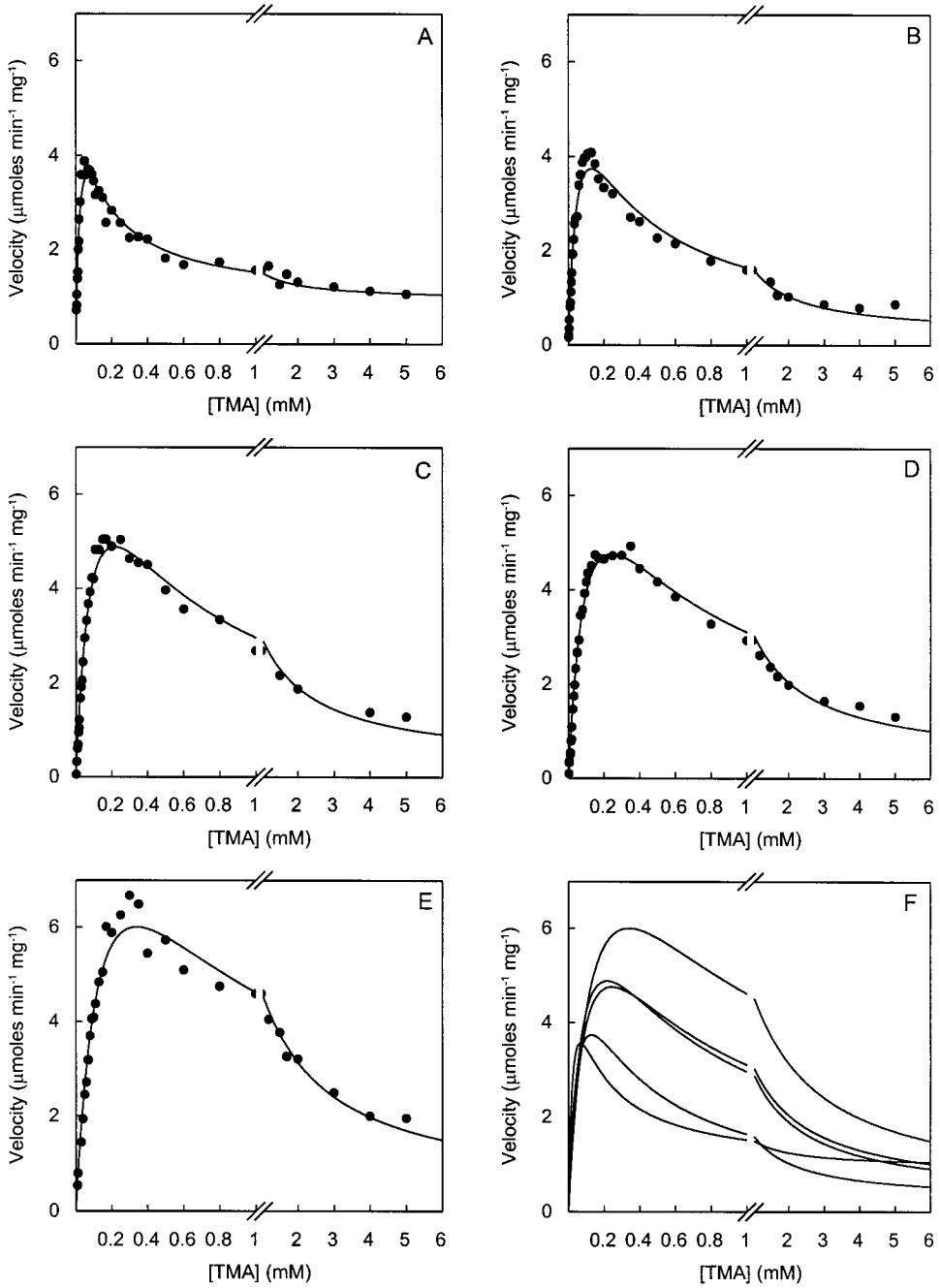

FIGURE 3: Plots of initial velocity against substrate concentration for reactions of TMADH with TMA and Fc^+. Reaction components were contained in 20 mM potassium phosphate buffer, pH 7, and the reactions were initiated by the addition of Fc^+. Assays were performed at 30 °C. Fc^+ concentrations are (A) 50 μM, (B) 100 μM, (C) 200 μM, (D) 300 μM, and (E) 400 μM. (F) Overlay of the fits for each data set shown in panels A−E. Data are fitted with eq 1.

to inhibit TMADH at high concentrations (Figure 4; Table 1); only *n*-butyldimethylamine (DMButA) did not display marked substrate inhibition. DMButA was therefore chosen for further spectroscopic analysis and comparison with the physiological reductant TMA (see below). Single-turnover stopped-flow studies of flavin reduction with DMButA as substrate revealed that flavin reduction is substantially compromised, even though the dissociation constant of the enzyme−substrate complex is reduced (Figure 5; Table 2). The latter finding is important since tight binding of the substrate by TMADH might affect partitioning between the 0/2 and 1/3 cycles of Scheme 1 (see Discussion). A prediction of Scheme 1 is that the rate of flavin reduction is not a factor responsible for partitioning between the two redox cycles. In agreement with this prediction, stopped-flow studies with TEA, for example, revealed it to be a very poor substrate (Figure 5; Table 2) but one that still gives clear steady-state inhibition (Figure 4).

Spectroscopic Analysis of TMADH during Steady-State Reactions with TMA. Stopped-flow studies of the reaction of TMADH with TMA have enabled deconvolution of the spectral forms of intermediates encountered in the reductive half-reaction (Figure 6). Four characteristic spectra are produced: that of the oxidized enzyme, two-electron reduced (dihydroquinone), two-electron reduced (flavin semiquinone and reduced iron-sulfur center), and the so-called spin-interacting state (*12*−*16*). The one- and three-electron reduced forms of TMADH are not observed in single-

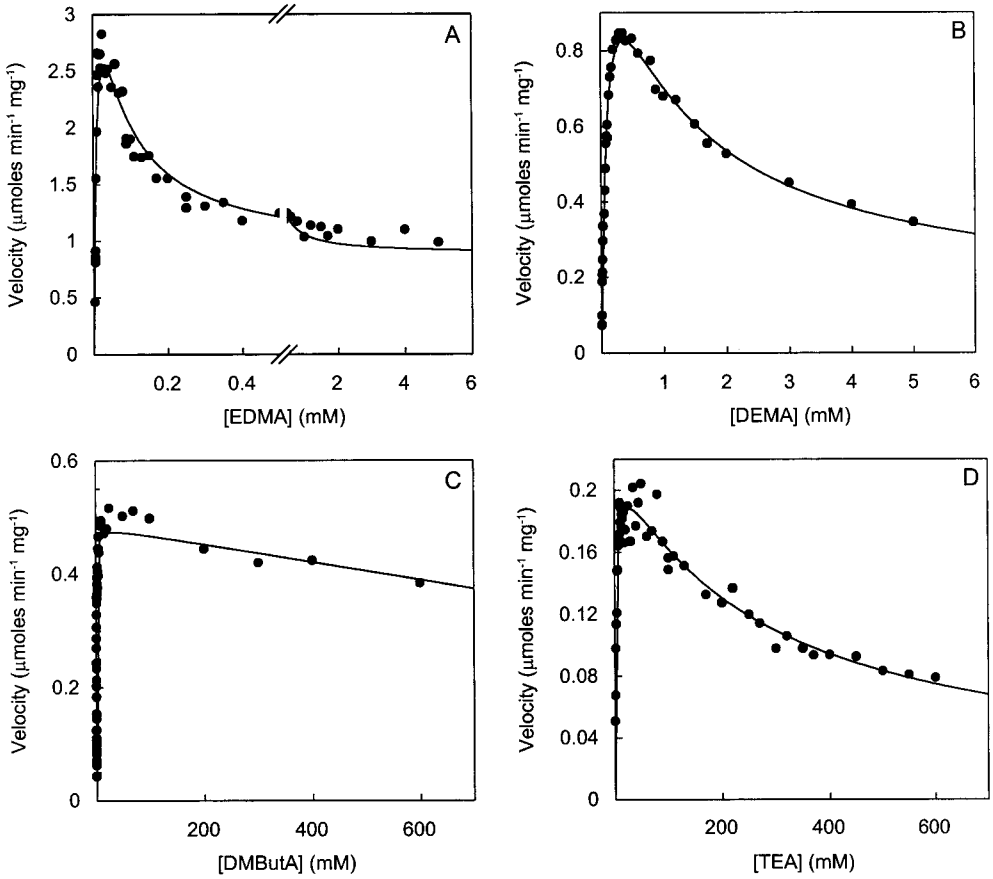

FIGURE 4: Plots of initial velocity against substrate concentration for reactions of TMADH with nonphysiological amines and Fc^+. Reaction conditions were as for Figure 3; Fc^+ concentration was 100 μM. (A) EDMA; (B) DEMA; (C) DMButA; (D) TEA. Data are fitted with eq 1.

Table 1: Steady-State Parameters for the Reaction of TMADH with Various Amine Substrates[a]

substrate	K_m (μM)	K_i (μM)	b	k_{cat} (s^{-1})	k_{cat}/K_m ($\times 10^3$) (M^{-1} s^{-1})
TMA	128 ± 16	120 ± 16	0.14 ± 0.01	40.5 ± 5	317 ± 79
EDMA	23.5 ± 3.8	25.3 ± 3.8	0.10 ± 0.02	23.7 ± 4	1009 ± 310
DEMA	111 ± 17	1009 ± 280	0.1 ± 0.03	3.8 ± 0.4	34.2 ± 8.4
TEA	2614 ± 330	25820 ± 6800	0.05 ± 0.09	0.6 ± 0.02	0.23 ± 0.04
DMButA	382 ± 20	$(2 \times 10^{11} \pm 8 \times 10^{12})$	$(7 \times 10^4 \pm 3 \times 10^6)$	0.11 ± 0.01	0.29 ± 0.005

[a] Reactions were performed in 20 mM potassium phosphate buffer, pH 7.0 at 30 °C, and were initiated by the addition of Fc^+. Fc^+ concentration was 100 μM. The poor ability of DMButA to inhibit TMADH in the high-substrate regime prevents meaningful evaluation of K_i and b for this substrate (figures are shown in parentheses). b is a factor that affects the intrinsic maximum velocity that would be obtained if the 1/3 cycle was not populated at saturating levels of substrate. K_m and k_{cat} values are apparent values, since eq 1 does take take into account Fc^+ concentration.

turnover studies, however, although they undoubtedly accumulate in the course of steady-state turnover.

Direct evidence for the operation of alternate redox cycles of the type shown (Scheme 1) was obtained by performing enzyme-monitored turnover experiments (*35*) with diode array detection in which TMADH was reacted in the stopped-flow with a mixture of TMA and Fc^+. In these turnover experiments, the concentration of TMADH was maintained at 4 μM, and Fc^+ was present at 100 μM. The reaction was monitored between 350 and 550 nm, the most informative region of the enzyme spectrum, where Fc^+ contributes little to the observed spectral change (Figure 1); reduction of Fc^+ can be monitored independently in the course of this experiment at 617 nm. Enzyme-monitored turnover experiments were performed over a range of TMA concentrations (20, 55, 100, and 500 μM and 2 mM) at 100 μM Fc^+. Depending on the TMA concentration, the minimum steady-state period observed extended over 5 s. As expected, the concentration of TMA profoundly affects the spectrum obtained during steady-state turnover. At high TMA concentrations (e.g., 500 μM and 2 mM), the spectrum exhibits a high absorption at 365 nm that is characteristic of the anionic flavin semiquinone (Figure 7, panels D and E). However, the relatively large absorption at 440 nm also indicates the iron−sulfur center of TMADH is substantially oxidized (compare with the spectrum of two-electron reduced TMADH with one electron in the flavin and one in the iron−sulfur center; Figure 6). The data therefore indicate that one-electron reduced TMADH (flavin semiquinone/oxidized iron−sulfur center) is the predominant species present during steady-state turnover at high concentrations of TMA. It is this form of TMADH that is predicted to accumulate during steady-state turnover in the 1/3 cycle of Scheme 1, concomitantly with the observation of excess substrate inhibition. In reactions performed at low concentrations of TMA (20 μM), on the other hand, the steady-state spectrum reflects

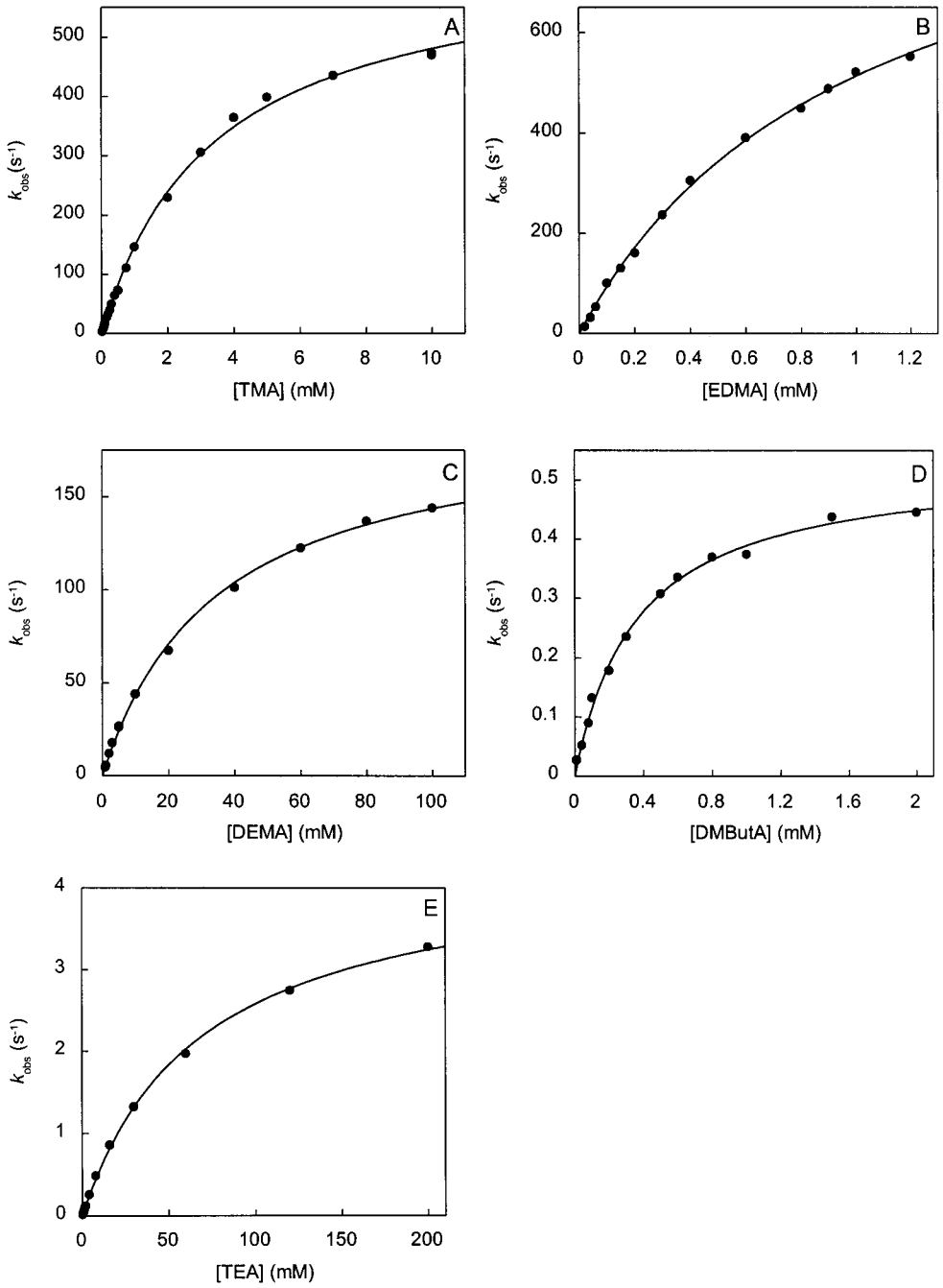

FIGURE 5: Plots of observed rate constants for flavin reduction against substrate concentration for reactions of TMADH with various amine substrates. Reactions were performed in 20 mM potassium phosphate buffer, pH 7.0 at 25 °C. Flavin reduction was monitored at 443 nm and data were fitted to eq 2. Enzyme−substrate dissociation constants and limiting rates for flavin reduction are given in Table 2.

Table 2: Kinetic Parameters for Flavin Reduction Determined by Stopped-Flow Analysis of the Reaction of TMADH with Various Amine Substrates

substrate	K_d (mM)	k_{red} (s^{-1})	k_{red}/K_d ($\times 10^3$) (M^{-1} s^{-1})
TMA	3.4 ± 0.2	643 ± 12	190 ± 12
EDMA	1.0 ± 0.1	1021 ± 35	1031 ± 98
DEMA	35 ± 2	193 ± 4	5.6 ± 0.4
TEA	70 ± 2	4.4 ± 0.1	0.06 ± 0.003
DMButA	0.36 ± 0.02	0.53 ± 0.01	1.5 ± 0.1

only a small quantity of anionic flavin semiquinone. Under these conditions the enhanced absorption at 365 nm seen at high TMA concentrations is lost (Figure 7, A). The steady-state spectrum is similar to that of oxidized TMADH (increased absorption at 443 nm and loss of signature at 365 nm), indicating that oxidized enzyme is the predominant species at low substrate concentrations. Clearly, in this regime, the 1/3 catalytic cycle does not predominate, and the majority of the catalytic throughput is through the 0/2 cycle. At intermediate TMA concentrations (55 and 100 μM) an intermediate situation is observed in which the 365 nm absorption indicative of the 1/3 cycle is present but is much less intense than that seen at high TMA concentrations (Figure 7B,C). Additionally, the 443 nm absorbance is higher than that seen with reactions performed with high concentrations of TMA. In this intermediate regime, therefore, both the 0/2 and 1/3 cycles appear to operate.

Upon reduction of the Fc^+ concentration to 50 μM, the absorbance spectrum of the enzyme indicates that anionic

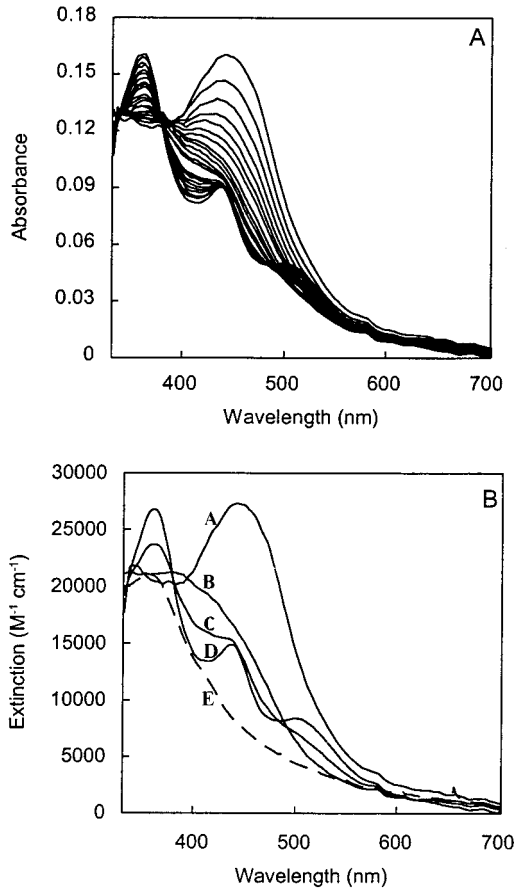

FIGURE 6: Time-dependent spectral changes for TMADH in single-turnover reactions with TMA. TMADH (7.5 μM) was rapidly mixed with TMA (125 μM) at pH 7.5. (A) Time-dependent spectral changes; the first spectrum is recorded 1.28 ms after mixing (for clarity, only selected subsequent spectra are shown). (B) Spectra of the intermediate forms during the course of the reductive half-reaction generated by global analysis and numerical integration methods with ProKin software (Applied Photophysics Ltd). Spectrum A, oxidized enzyme; spectrum B, two-electron reduced enzyme (dihydroflavin); spectrum C, two-electron reduced enzyme (flavin semiquinone and reduced iron−sulfur center); spectrum D, spin-interacting state of TMADH. The spectral changes are shown for a single-turnover reaction at pH 7.5 rather than pH 7.0 because at the latter pH value the flavin reduction and internal electron transfer steps are not fully resolved, leading to kinetic mixing effects (*19*). Under these conditions the spectral forms of the intermediate redox states cannot be deconvoluted. The spectrum of three-electron reduced TMADH (generated under anaerobic conditions by titration with sodium dithionite) is illustrated (dashed spectrum).

flavin semiquinone/oxidized iron−sulfur center are the predominant redox states present in TMADH at all TMA concentrations investigated (20 μM, 500 μM, and 2 mM; Figure 7F). In other words, the switch from the 1/3 cycle to the 0/2 cycle (Scheme 1) that is seen with 100 μM Fc^+ does not occur when the Fc^+ concentration is reduced to 50 μM. The data thus indicate that partitioning between the two redox cycles is critically dependent on both TMA and Fc^+ concentration, as predicted by Scheme 1, and demonstrate that as the ratio of reducing to oxidizing substrate increases, the level of enzyme reduction in the steady-state also increases.

Spectroscopic Analysis of TMADH during Steady-State Reactions with DMButA. Steady-state assays demonstrated that the inhibition seen with DMButA is much less marked than that by other substrates (see above). Enzyme-monitored turnover experiments were therefore of interest, to ascertain whether the 0/2 cycle predominated to a greater extent than is seen with TMA in the experiments above. Reactions were performed with 100 μM Fc^+ and over a range of DMButA concentrations (100 μM, 20 mM, and 200 mM). In all cases, the spectra obtained during steady-state turnover show only incomplete development of the 365 nm absorption of the anionic semiquinone compared to the results obtained with TMA and a 440 nm absorbance similar to that of oxidized TMADH (Figure 8). Clearly, with DMButA as substrate the 1/3 cycle is populated to only a small extent during steady-state turnover and the majority of substrate oxidation occurs exclusively via the 0/2 cycle. This analysis thus provides an explanation for the lack of marked substrate inhibition seen with this nonphysiological substrate in the high-concentration regime.

Single-Wavelength Enzyme-Monitored Turnover Experiments. To more effectively correlate the properties of the enzyme in the steady state, enzyme-monitored turnover experiments were performed in which 4 μM enzyme was reacted with 100 μM Fc^+ and varying concentrations of TMA over the range 250 μM−2.0 mM (all concentrations after mixing). The reaction was followed at three wavelengths: 443 nm, monitoring the net level of enzyme reduction; 365 nm, monitoring the accumulation of the anionic flavin semiquinone in the course of the steady state; and 617 nm, monitoring the enzyme-catalyzed reduction of Fc^+ in the course of the reaction. The data are shown in Figure 9, where several qualitative trends are evident. First, excess substrate inhibition is manifested as a decrease in the slope of the 617 nm transients as the concentration of TMA increases and also in the trend toward longer time excursions as the [TMA] increases—as expected, it takes the enzyme longer to consume the (limiting) 100 μM Fc^+ at the higher concentrations of TMA. Second, an increased accumulation in anionic semiquinone in the steady state as [TMA] increases is evident as a loss of the pronounced bowing in the 365 nm transients in going from 250 μM to 2.0 mM TMA. This is more evident in a comparison of the excursions at 365 nm as a function of [TMA], as shown in Figure 10. The principal observation is that, as the model predicts, there is a substantial increase in the amount of semiquinone that accumulates in the steady state as the [TMA] increases. A comparison of the areas under the curves for the excursions at 365 nm indicates that the amount of semiquinone accumulating and persisting in the steady-state more than doubles in going from 250 μM to 2.0 mM. It is significant that the model in fact predicts this increased accumulation of flavin semiquinone at concentrations of TMA where excess substrate inhibition is observed.

An analysis of the transients at 443 nm at short time intervals permits an examination of the approach of the system to the steady-state. As shown in Figure 11, this approach to the steady state is increasingly rapid as the [TMA] increases, as expected given the known behavior of the fast phase of the reaction of enzyme with both DEMA and TMA (*17*, *19*). A transient "overreduction" of the enzyme is observed at all concentrations of TMA, due to the initial reduction of the flavin in the fast phase of the first turnover. This overshoot of the steady-state level of enzyme reduction increases with [TMA] as the reaction of enzyme with substrate in the first turnover goes increasingly

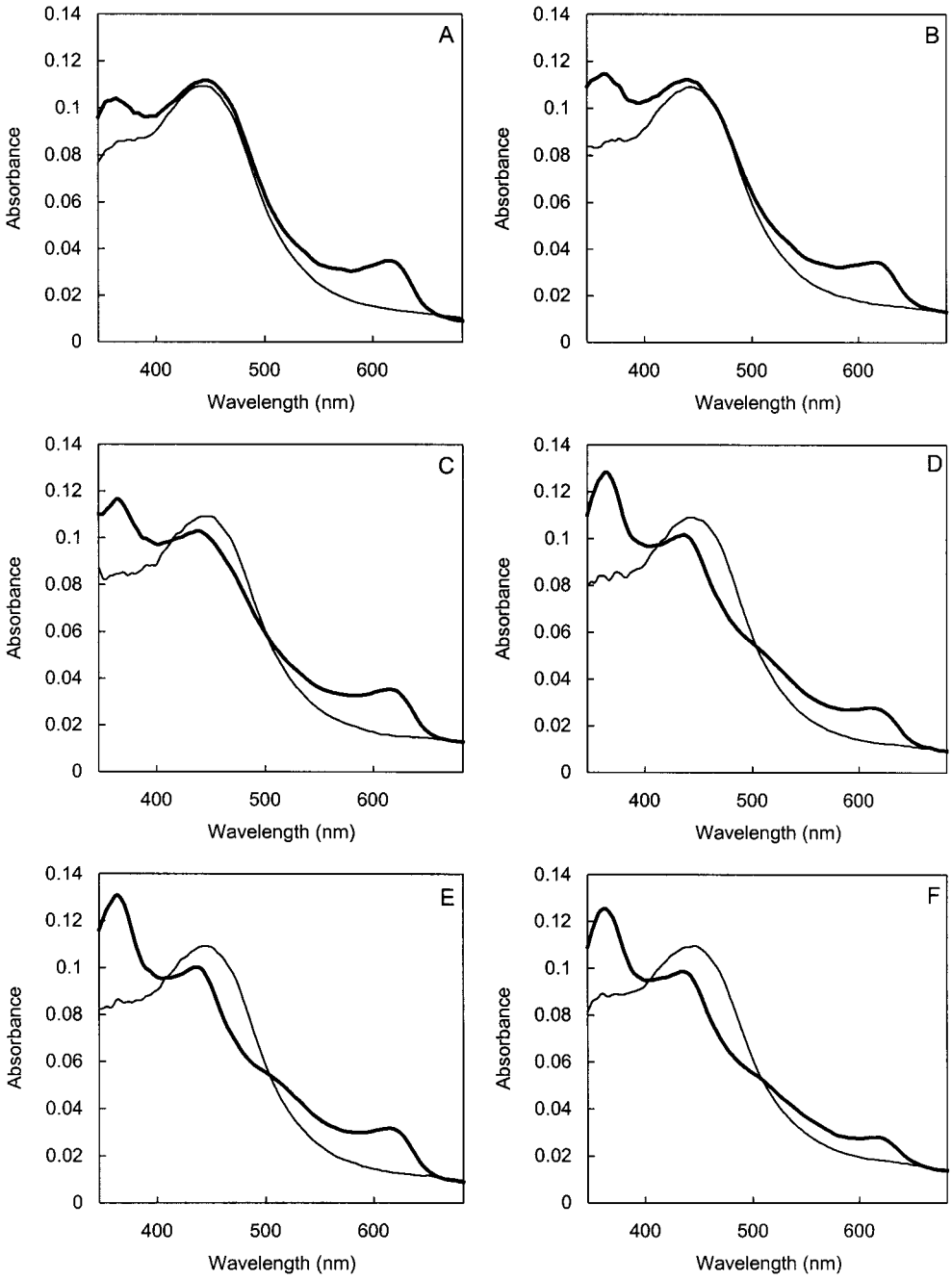

FIGURE 7: Spectral forms of TMADH observed during steady-state turnover with TMA and Fc^+. For reference, in all panels the spectrum of oxidized enzyme is indicated by the thinner line. (A) Steady-state spectrum (thick line) observed in the presence of 20 μM TMA and 100 μM Fc^+; (B) steady-state spectrum (thick line) observed in the presence of 55 μM TMA and 100 μM Fc^+; (C) steady-state spectrum (thick line) observed in the presence of 100 μM TMA and 100 μM Fc^+; (D) steady-state spectrum (thick line) observed in the presence of 500 μM TMA and 100 μM Fc^+; (E) steady-state spectrum (thick line) observed in the presence of 2 mM TMA and 100 μM Fc^+; (F) steady-state spectrum (thick line) observed in the presence of 20 μM TMA and 50 μM Fc^+. All reactions were performed in 20 mM potassium phosphate buffer, pH 7.0 at 25 °C.

to completion prior to entering the steady state, yielding the full absorbance change associated with reduction of the enzyme flavin. The rate constants obtained from this pre-steady-state portion of the 443 nm transients are 50 s^{-1}, 116 s^{-1}, and 286 s^{-1} at 100 μM, 500 μM, and 2 mM TMA, respectively. These values are entirely consistent with the observed rate constants for flavin reduction obtained from single-turnover stopped-flow studies (Figure 5). Once the steady state has been achieved, the absorbance at 443 nm rebounds considerably, reflecting a higher net level of oxidation in the steady state than the initial two-electron reduced form generated in the course of the fast phase of the first turnover.

A major advantage of the enzyme-monitored turnover experiments is that they permit a quantitative comparison of turnover and the status of the enzyme in the course of the steady state, and in particular a comparison of k_{cat} from the ΔA at 617 nm (following Fc^+ reduction explicitly) with that which can be obtained from the transients at 443 nm. Gibson et al. (*35*) have shown that for transients of the type seen at 443 nm in the present experiments, the area under the curve is proportional to the total concentration of limiting substrate

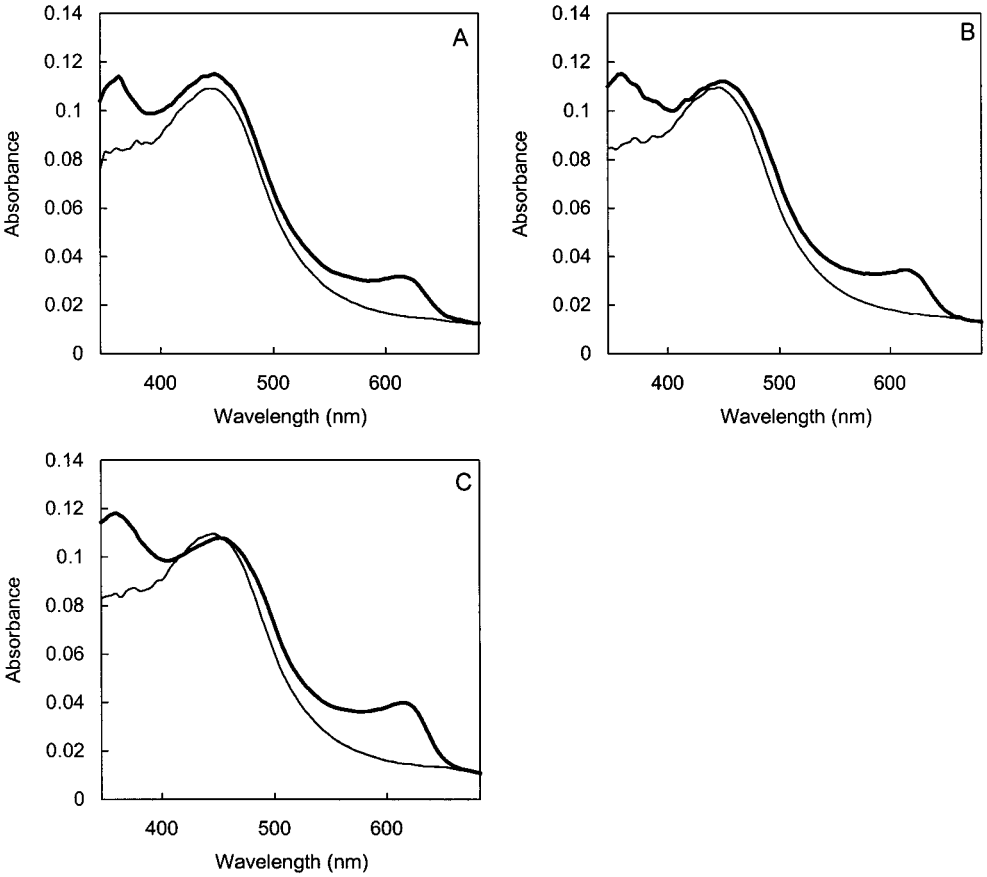

FIGURE 8: Spectral forms of TMADH during steady-state turnover with DMButA. For reference, in all panels the spectrum of oxidized enzyme is indicated by the thinner line. (A) Steady-state spectrum (thick line) observed in the presence of 100 μM DMButA and 100 μM Fc^+; (B) steady-state spectrum (thick line) observed in the presence of 2 mM DMButA and 100 μM Fc^+; (C) steady-state spectrum (thick line) observed in the presence of 200 mM DMButA and 100 μM Fc^+. All reactions were performed in 20 mM potassium phosphate buffer, pH 7.0 at 25 °C.

(in this case, Fc^+, at 100 μM). Turnover numbers at any point in the course of the transient can be obtained from the ratio of the area under the curve over any specific time interval to that of the total curve, yielding the consumption of oxidizing substrate (in the present case) per unit time. Table 3 shows the values for k_{cat} obtained over two time intervals in the transients: between 1 and 2 s and for a 1 s interval in the middle of the steady-state as determined by the 443 nm transient (the initial velocity value from the 617 nm transients over the 0−1 s interval are also given). Interestingly, there is a significant discrepancy between the 617 nm and enzyme-monitored turnover values for k_{cat} for the 1−2 s interval, particularly at the lower [TMA] concentrations (compare the values in columns 3 and 5 of Table 3). This discrepancy largely vanishes by the midpoint of the steady state, however, to within the error of the measurement in all likelihood (columns 4 and 6). This trend is evident in the transients themselves (Figure 9), as the 617 nm transient is distinctly bowed in the steady-state region (particularly at low [TMA]), whereas the absorbance at 443 nm changes relatively little in this region until the Fc^+ has been consumed at the end of the steady state. Again, this bowing in the 617 nm transients becomes significantly less pronounced at higher [TMA]. The 617 nm absorbance change must reflect the actual enzyme turnover, but the 443 nm transients better define the duration of the steady state. What the data indicate quite clearly is that over the course of the steady state, catalytic throughput decreases significantly, particularly at lower [TMA], precisely what the model predicts as the system switches over from the more efficient 0/2 cycle to the less efficient 1/3 cycle.

DISCUSSION

In this paper, we have attempted to correlate the known effects of substrate and inhibitor binding with the mechanism of inhibition of TMADH by substrate under steady-state conditions. Previous studies with TMADH have demonstrated an interaction between the FMN and 4Fe-4S centers that is profoundly influenced by binding of substrate or the substrate analogue TMAC (*13*, *16*). The distribution of the reducing equivalents within two-electron reduced TMADH is known to be influenced strongly by substrate and pH: for dithionite-reduced enzyme at low pH (pH 6), the distribution favors dihydroflavin and oxidized 4Fe-4S center (*18*); at high pH (pH 10), formation of flavin semiquinone and reduced 4Fe-4S center is favored, with the magnetic moments of the two paramagnetic centers interacting strongly to give a spin-interacting state (triplet state), which is distinguished by a complex EPR signal centered near $g \sim 2$ and an unusually intense half-field $g \sim 4$ signal (*12*−*16*, *18*, *36*). In addition, binding of the substrate analogue TMAC is known to perturb the reduction potentials of the flavin center. On binding TMAC, the potential for the quinone/semiquinone couple increases from +44 mV to +240 mV at pH 7.0 (*24*, *37*), while that of the semiquinone/hydroquinone couple decreases from +36 to −50 mV. The effect is not simply to stabilize

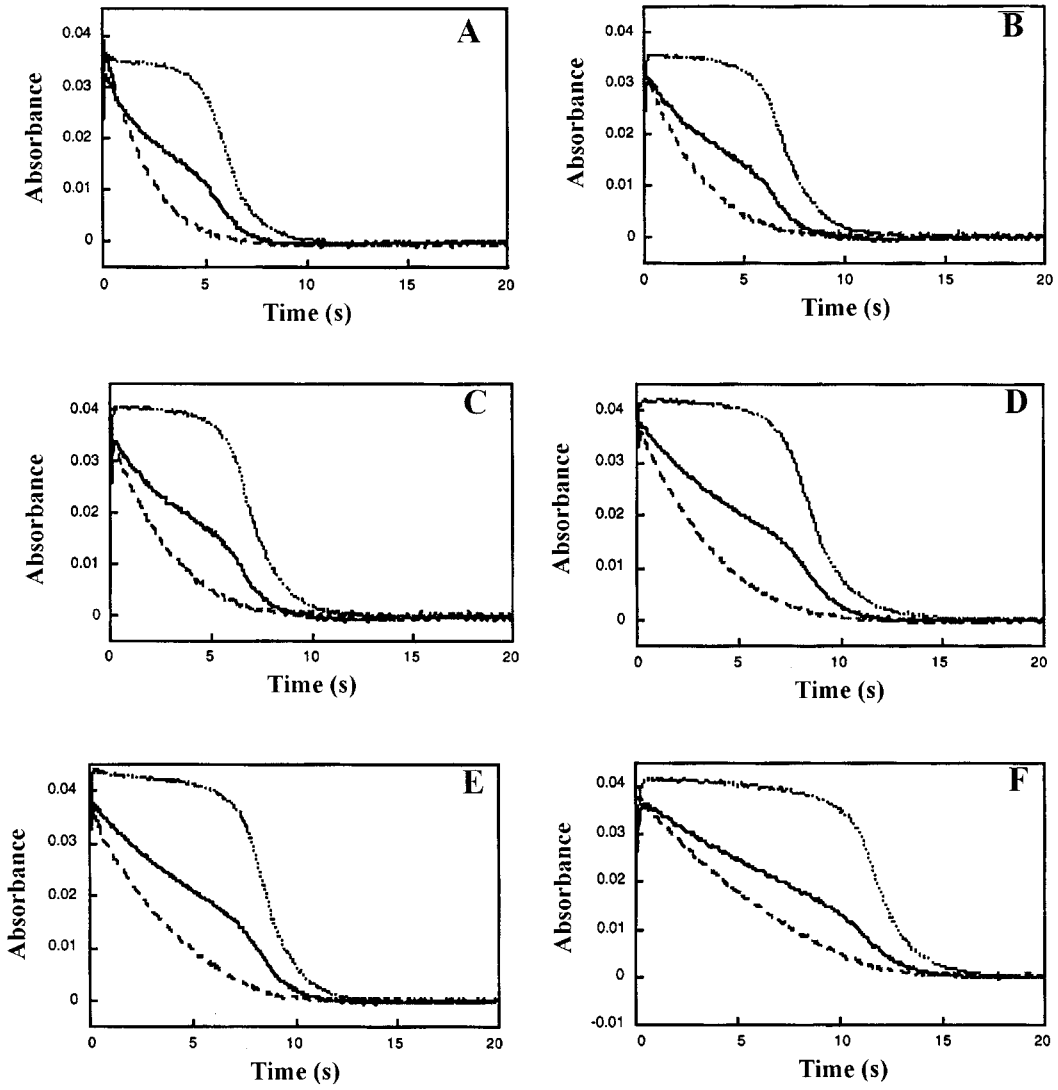

FIGURE 9: Transients obtained from enzyme-monitored turnover experiments. All reactions were performed in 20 mM potassium phosphate buffer, pH 7.0 at 25 °C. TMA concentrations were (A) 250 μM TMA, (B) 300 μM, (C) 400 μM, (D) 500 μM, (E) 1 mM, and (F) 2 mM. In all panels: upper transient, 443 nm; central transient, 365 nm; lower transient, 617 nm.

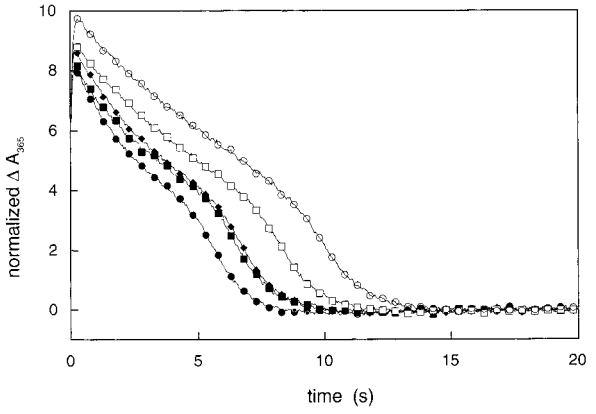

FIGURE 10: Normalized transients seen at 365 nm in the course of turnover. Reaction conditions are the same as in Figure 9. Trimethylamine concentrations were 250 μM (●), 400 μM (■), 500 μM (◆); 1.0 mM (△), and 2.0 mM (○). The increased accumulation of anionic semiquinone at high [TMA] is evident from the larger integrated area under the curves as the concentration of TMA is increased.

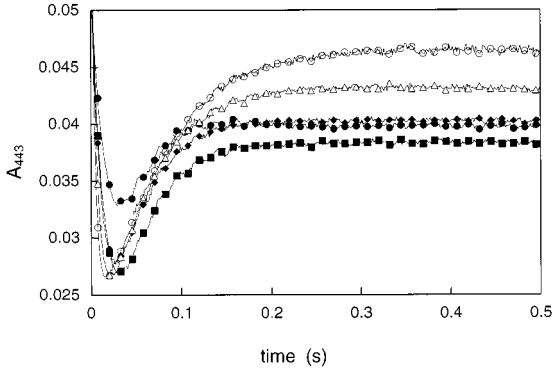

FIGURE 11: Short-time absorbance changes at 443 nm in the course of turnover. Reaction conditions are the same as in Figure 9; trimethylamine concentrations are as in Figure 10. The increased absorbance at 0.5 s in going from 400 μM to 2.0 mM reflects the increasingly oxidized state of the enzyme as the reductive half-reaction slows down in the [TMA] regime where excess substrate inhibition is observed.

the semiquinone oxidation state of the flavin but to alter its value relative to the potential of the iron−sulfur center. At pH 7.0, this potential is +102 mV in the absence of TMAC and +50 mV in its presence. Binding of TMAC (and by inference also TMA) is thus expected to significantly perturb the oxidation−reduction equilibrium between flavin and Fe/S in the one-electron reduced enzyme, shifting the equilibrium

Table 3: Steady-State Kinetic Parameters Determined from Quantitative Analysis of Enzyme-Monitored Turnover Experiments[a]

	turnover number (s^{-1})				
[TMA]	$k_{cat}^{617\ nm_0}$	$k_{cat}^{617\ nm_1}$	$k_{cat}^{617\ nm_2}$	$k_{cat}^{emt_1}$	$k_{cat}^{emt_2}$
250 μM	9.9	5.8	4.0	4.3	4.2
300 μM	7.9	4.9	3.6	4.3	4.0
400 μM	6.3	4.0	3.0	3.5	3.5
500 μM	4.6	3.8	2.5	2.7	2.6
1.0 μM	4.8	3.4	2.5	2.8	2.7
2.0 μM	2.9	2.9	2.0	2.3	2.2

[a] Reactions were performed in 20 mM potassium phosphate buffer, pH 7.0 at 25 °C. TMADH concentration was 4 μM and Fc^+ concentration was 100 μM. $k_{cat}^{617\ nm_0}$, turnover number calculated from the initial velocity of the 617 nm transient in the 0−1 s range; $k_{cat}^{617\ nm_1}$, turnover number calculated for the 617 nm transient in the 1−2 s range; $k_{cat}^{617\ nm_2}$, turnover number calculated for the 617 nm transient from a 1 s interval in the middle of the steady-state period as determined by the 443 nm transient; $k_{cat}^{emt_1}$, enzyme-monitored turnover number calculated from the 443 nm transient in the 1−2 s range; $k_{cat}^{emt_2}$, enzyme-monitored turnover number calculated from the 443 nm transient for a 1 s interval in the middle of the steady-state period.

from a position favoring Fe/S reduction by approximately 10:1 to one favoring essentially quantitative formation of the flavin semiquinone. To the extent that this occurs, the enzyme will not be able to oxidize the bound substrate as the flavin is in the wrong oxidation state. The substrate-bound one-electron reduced intermediate is unique to the 1/3 catalytic cycle, and this effect is thus expected to compromise catalysis by this cycle.

The spectroscopic and potentiometric data for wild-type TMADH provide a framework for rationalizing the observed steady-state behavior of the enzyme. Previous workers have proposed a second substrate binding site in the enzyme whose occupation leads to substrate inhibition by attenuating internal electron transfer from the flavin to the 4Fe-4S center (*20*, *38*). However, the X-ray structure of TMADH in complex with TMAC provides no evidence for a second binding site (*21*, *22*), and studies with ^{14}C TMA reveal that no more than 1 equiv of substrate is bound to the reduced enzyme (*16*). Additionally, and in support of a single TMA-binding site, our recent EPR studies have revealed that only 1 equiv of TMAC is required to generate the spin-interacting state in two-electron reduced TMADH (*19*). An alternative explanation for excess substrate inhibition has been proposed (*23*) in which catalysis occurs via alternate 0/2 and 1/3 catalytic cycles (Scheme 1). Turnover via the 1/3 cycle is expected to predominate at high concentrations and, as discussed above, is expected to be slower because of the unfavorable effect of substrate on flavin reduction potential.

Using Fc^+ as oxidizing substrate, which we have demonstrated to react with TMADH at the Fe/S center (as does ETF), we have examined the reduction levels of the 6-*S*-cysteinyl FMN and 4Fe-4S center in TMADH under steady-state conditions. These studies demonstrate that a one-electron reduced enzyme species containing the anionic semiquinone form of the 6-*S*-cysteinyl FMN and oxidized 4Fe-4S center predominates under steady-state conditions in the presence of high concentrations of substrate, whereas at low substrate concentrations oxidized TMADH is the predominant form. We have also shown that some other substrates for TMADH (e.g., EDMA, DEMA, and TEA) also exhibit excess substrate inhibition. Our stopped-flow studies reveal that the limiting rates for flavin reduction with some of these substrates (e.g., DEMA and particularly TEA) are substantially reduced compared with TMA. Consequently, and as predicted by Scheme 1, the rate of flavin reduction per se does not account for partitioning into the slower 1/3 cycle. Instead, predominance of the 1/3 cycle depends on the ability of substrate to bind to enzyme possessing the flavin semiquinone rather than the oxidized form (as reflected in the perturbation of flavin reduction potential upon binding of substrate). Binding of substrate to enzyme containing the flavin semiquinone perturbs the reduction potential of the oxidized/semiquinone flavin couple (thereby shifting the electron distribution within one-electron reduced enzyme in favor of semiquinone formation). Clearly, over the range of substrate concentrations used in this study, DEMA, EDMA, and TEA are able to bind and perturb the flavin potential of one-electron reduced enzyme. Interestingly, DMButA binds relatively tightly to oxidized TMADH (K_d = 0.36 mM; Table 2) and has the greatest affinity for oxidized TMADH of all the substrates included in this study. However, the lack of marked inhibition seen in the steady state with DMButA suggests this substrate binds less well to reduced forms of the enzyme as compared to TMA. The expectation, therefore, that the anionic flavin semiquinone does not accumulate appreciably during steady-state turnover at all DMButA concentrations studied is consistent with the results of our enzyme-monitored turnover experiments. This situation may be similar to that presumed for the Y169F mutant TMADH, which does not show inhibition with the physiological substrate TMA (*39*). In this latter case, negative charge cannot develop on the side chain of Phe-169 on binding substrate to one-electron reduced enzyme. Thus, the reduction potential of the semiquinone/oxidized flavin couple in the Y169F mutant TMADH should not be perturbed in the manner described for the wild-type enzyme. Work is in progress to determine the reduction potentials of the Y169F mutant TMADH (in the presence and absence of TMAC) to establish further the link between substrate binding, electronic redistribution in the flavin, formation of the spin-interacting state, and enzyme inhibition in the high-substrate regime.

CONCLUSIONS

The steady-state kinetic mechanism of wild-type TMADH comprises two alternating redox cycles and the partitioning between these cycles is dependent on the concentration of reducing substrate and the electron acceptor. This bifurcated kinetic scheme accounts for the observed inhibition of TMADH at high concentrations of substrate without invoking a second, inhibitory substrate binding site. The 1/3 cycle predominating at high [TMA] is catalytically compromised due to the unfavorable position of the equilibrium between the two redox-active centers in the substrate-bound, one-electron reduced enzyme (boxed in Scheme 1). Binding of substrate to one-electron reduced enzyme leads to the accumulation of a flavin semiquinone/oxidized 4Fe-4S intermediate in the so-called 1/3 redox cycle, leading to inhibition in the high substrate regime. Excess substrate inhibition is in fact a necessary consequence of the shift in the reduction potential of the flavin and 4Fe-4S centers in one-electron reduced enzyme upon binding substrate and substrate analogues.

REFERENCES

1. Steenkamp, D. J., and Mallinson, J. (1976) *Biochim. Biophys. Acta 429*, 705−19.
2. Steenkamp, D. J., and Singer, T. P. (1976) *Biochem. Biophys. Res. Commun. 71*, 1289−95.
3. Steenkamp, D. J., McIntire, W., and Kenney, W. C. (1978) *J. Biol. Chem. 253*, 2818−24.
4. Steenkamp, D. J., Kenney, W. C., and Singer, T. P. (1978) *J. Biol. Chem. 253*, 2812−7.
5. Hill, C. L., Steenkamp, D. J., Holm, R. H., and Singer, T. P. (1977) *Proc. Natl. Acad. Sci. U.S.A. 74*, 547−51.
6. Kasprzak, A. A., Papas, E. J., and Steenkamp, D. J. (1983) *Biochem. J. 211*, 535−41.
7. Lim, L. W., Mathews, F. S., and Steenkamp, D. J. (1988) *J. Biol. Chem. 263*, 3075−8.
8. Scrutton, N. S. (1994) *BioEssays 16*, 115−122.
9. Steenkamp, D. J., and Gallup, M. (1978) *J. Biol. Chem. 253*, 4086−9.
10. Duplessis, E. R., Rohlfs, R. J., Hille, R., and Thorpe, C. (1994) *Biochem. Mol. Biol. Int. 32*, 195−199.
11. Byron, C. M., Stankovich, M. T., Husain, M., and Davidson, V. L. (1989) *Biochemistry 28*, 8582−8587.
12. Steenkamp, D. J., Singer, T. P., and Beinert, H. (1978) *Biochem. J. 169*, 361−9.
13. Steenkamp, D. J., Beinert, H., McIntire, W. S., and Singer, T. P. (1978) in *Mechanisms of oxidizing enzymes* (Singer, T. P., and Ondarza, R. N., Eds.) pp 127−141, Elsevier North-Holland Inc, New York.
14. Singer, T. P., Steenkamp, D. J., Kenney, W. I. C., and Beinert, H. (1980) in *Flavins and Flavoproteins* (Yagi, K., and Yamano, T., Eds.) pp 277−287, Japan Scientific Societies Press, Tokyo.
15. Steenkamp, D. J., and Beinert, H. (1982) *Biochem. J. 207*, 241−52.
16. Steenkamp, D. J., and Beinert, H. (1982) *Biochem. J. 207*, 233−9.
17. Rohlfs, R. J., and Hille, R. (1994) *J. Biol. Chem. 269*, 30869−79.
18. Rohlfs, R. J., and Hille, R. (1991) *J. Biol. Chem. 266*, 15244−52.
19. Jang, M.-H., Basran, J., Scrutton, N. S., and Hille, R. (1999) *J. Biol. Chem. 274*, 13147−13154.
20. Falzon, L., and Davidson, V. L. (1996) *Biochemistry 35*, 2445−52.
21. Lim, L. W., Shamala, N., Mathews, F. S., Steenkamp, D. J., Hamlin, R., and Xuong, N. H. (1986) *J. Biol. Chem. 261*, 15140−6.
22. Bellamy, H. D., Lim, L. W., Mathews, F. S., and Dunham, W. R. (1989) *J. Biol. Chem. 264*, 11887−92.
23. Huang, L., Rohlfs, R. J., and Hille, R. (1995) *J. Biol. Chem. 270*, 23958−65.
24. Stankovich, M. T., and Steenkamp, D. J. (1987) in *Flavins and Flavoproteins* (Edmondson, D. E., and McCormick, D. B., Eds.) pp 687−690, Walter de Gruyter, Berlin.
25. Hille, R., and Stewart, R. (1984) *J. Biol. Chem. 259*, 1570−1576.
26. Lehman, T. C., Hale, D. E., Bhala, A., and Thorpe, C. (1990) *Anal. Biochem. 186*, 280−284.
27. Wilson, E. K., Mathews, F. S., Packman, L. C., and Scrutton, N. S. (1995) *Biochemistry 34*, 2584−91.
28. Wilson, E. K., Huang, L., Sutcliffe, M. J., Mathews, F. S., Hille, R., and Scrutton, N. S. (1997) *Biochemistry 36*, 41−8.
29. Scrutton, N. S., Packman, L. C., Mathews, F. S., Rohlfs, R. J., and Hille, R. (1994) *J. Biol. Chem. 269*, 13942−50.
30. Leatherbarrow, R. J. (1992) Grafit v3, Erithacus Software Ltd, Staines, U.K.
31. Segel, I. H. (1975) *Enzyme Kinetics*: *Behavior and analysis of rapid equilibrium and steady-state enzyme systems*, Wiley-Interscience, New York.
32. Craig, D. H., Moody, P. C. E., Bruce, N. C., and Scrutton, N. S. (1998) *Biochemistry 37*, 7598−607.
33. Strickland, S., Palmer, G., and Massey, V. (1975) *J. Biol. Chem. 250*, 4048−4052.
34. Nagy, J., Kenney, W. C., and Singer, T. P. (1979) *J. Biol. Chem. 254*, 2684−8.
35. Gibson, Q. H., Swoboda, B. E. P., and Massey, V. (1964) *J. Biol. Chem. 239*, 3927−3934.
36. Rohlfs, R. J., Huang, L., and Hille, R. (1995) *J. Biol. Chem. 270*, 22196−207.
37. Pace, C. P., and Stankovich, M. T. (1991) *Arch. Biochem. Biophys. 287*, 97−104.
38. Falzon, L., and Davidson, V. L. (1996) *Biochemistry 35*, 12111−8.
39. Basran, J., Sutcliffe, M. J., Hille, R., and Scrutton, N. S. (1999) *J. Biol. Chem. 274*, 13155−13161.

BI9914098